Journal of Education For Pure Science- University of Thi-Qar
Vol.9, No.1 (March 2019)
Website: jceps.utq.edu.iq *Email: jceps@eps.utq.edu.iq*

DOI: http://doi.org/10.32792/utq.jceps.09.01.24

TiO_2/NiO-RGO Nanocomposite As Effective Photoanode For Improving Performance Of Dye Sensitized Solar Cells

Hawraa M. khudier[1], Majid R. Al-bahrani[1]

[1]Faculty of Science, University of Thi-Qar, Thi-Qar, Iraq.

Abstract:

The photoanode of dye sensitized solar cells (DSSCs) have been fabricated as a double mixture where nickel-oxide (NiO), graphene-oxide (RGO) inserted with titanium-dioxide (TiO_2) using simple chemical methods the sample is coated on FTO glass by doctor-blade method using platinum as counter electrode. After constructing TiO_2/NiO-RGO photoanode, the photoanode has shown enhanced light adsorption properties, faster electron transport, lower internal resistances and lower charge recombination rate, which resulted in high current density. The results exhibit much better conversion efficiency in comparison to the DSSCs with pure TiO_2 and with TiO_2/ RGO PE

Keywords: Dye-sensitized solar cells, graphene-oxide/TiO_2, nickel-oxide (NiO), titanium-dioxide (TiO_2), Photoanode.

1. Introduction

A new technique has been used to manufacture solar cells known as dye-sensitized solar cell, which is the solar cell manufactured by organic pigments, is known as DSSC which is a new technology under the future technologies for the solar cell industry at a low cost. Cells are made of semiconductor material between an anode and electrolyte .A substance that contains ions that make the material conductive to electricity. This technology was invented by Michael Gratzel and O'Regan in 1991 and they are also known as Gratzel cells [1]Since then, many workers have been extensively investigating this DSSCs using various metal complex sensitizers. Several metal oxide materials have been explored for the photoanode such as TiO_2[2]–[5].Zno[6]–[8].NiO[9], [10].RGO[11]–[13].CuO[14], [15].Among these materials TiO_2 compact layer receives much discussion becouse it can improved performance of DSSC .

Graphene/TiO_2 composite layer and a TiO2 nanoparticles (P25) under layer used as photo anode in 2018 after construction of double layer photoanode with proper amount of graphene .The DSSC exhibited a Voc of 0.72 V, Jsc of 15.01 mA cm^{-2}, and FF of 0.66 with the energy conversion efficiency of 7.08% in 2018 [11].

DSSCs are consisting three major parts: First part is photo anode which absorber the incident light, generates free electrons and transfers the electrons to the external circuit. The counter electrode is the second part which conducts the electrons from the external circuit back to the electrolyte of the cell .The third part is electrolyte which carries the electrons back to the photo anode to complete the electron circulation. The photoanode of a DSSC is generally composed of TiO_2 layer coated on a transparent conducting glass or plastic substrate that is brought together in a sandwich like architecture [16],[17], [18]as show in figure(1).

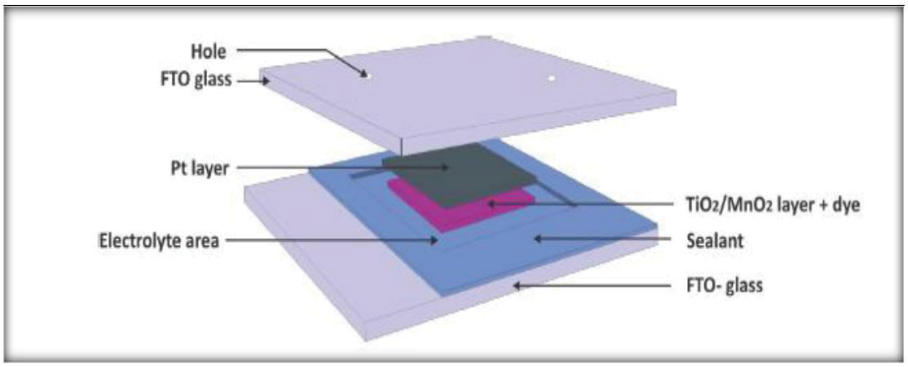

Figure1: sandwich like structure for DSSC[19]

In brief the basic sequence of events in DSSCs is as the following equations:

$$TiO_2/Dye \longrightarrow TiO_2+Dye^* \quad (1)$$

$$TiO_2/Dye^* \longrightarrow TiO_2/Dye^+ + e^-(TiO_2) \quad (2)$$

$$e^-(TiO_2) \longrightarrow e^-(FTO) \quad (3)$$

$I_3^- + 2e^-$ (Pt) $\longrightarrow$ $3I^-$ (4)

$1.5I^- + TiO_2/Dye+ \longrightarrow 0.5I_3^- + TiO_2/Dye$ (5) [18]

The photon incident on the cell is absorbed by the organic dye, which stimulates the electron from the ground state to the excited state of dye (Dye^*). The exited electrons injected in to the CB of TiO_2 then assemble in FTO glass after passing through an external circuit, the electron is reintroduced into the DSSC at the Pt CE. The electrolyte gives an electron to the dye to fill the hole (Dye^+) and complete the circuit as shown in fig (2) the efficiency of a DSSC depends on four energy levels of the component: the excited state (approximately LUMO) and the ground state (HOMO) of the photosensitizer, the Fermi level of the TiO_2 electrode and the redox potential of the mediator (I^-/I_3^-) in the electrolyte [20]

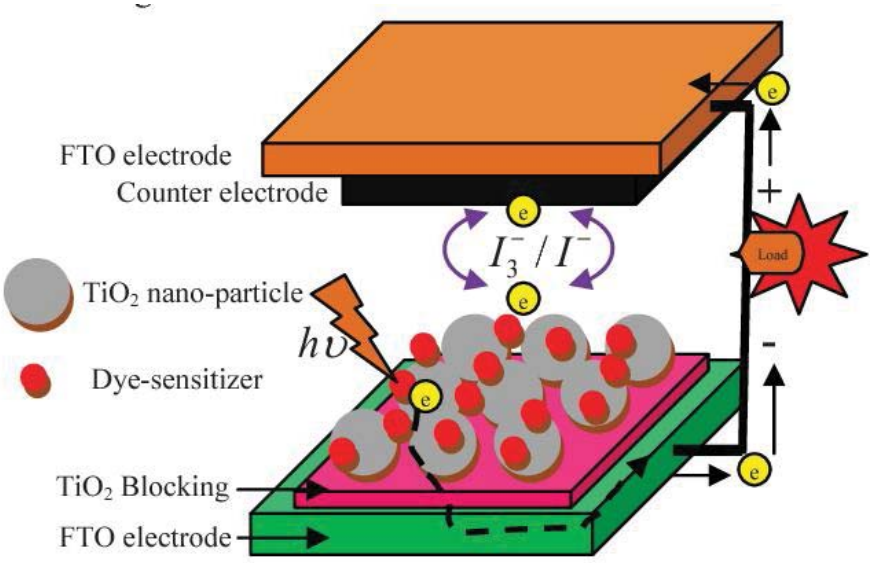

Fig(2): The simple structure and operation of DSSC[13].

In this study (DSSCs) have been designed and manufactured based on nanoparticles of titanium dioxide (TiO_2) paste deposition on fluorine doped tin oxide (FTO) glass using doctor-blade method ..For counter electrode Pt were coated on FTO conductive glass, iodide/tri-iodide (I^-/I_3^-) used as electrolyte and finally combine the two electrodes together in
a sandwich manner then injected the electrolyte between them. Nickel oxide and graphene oxide were then added to TiO_2 of Photoanode with simple chemical methods to improve the performance of DSSC. Figure (3) shows the cells we designed in this work

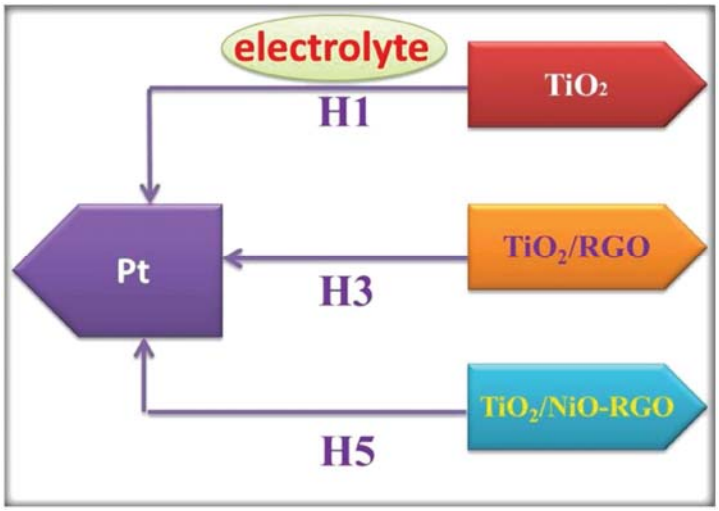

Figure (3): Schematic illustration DSSCs based on the TiO_2 nanoparticle, TiO_2/RGO and TiO_2/NiO-RGO as photo electrode.

2. Experimental part:

2.1 Chemicals and Materials

In this paper, the materials and solvents were purchased from Sino pharm Chemical Reagent Company. titanium (IV) isopropoxide (TIP) were purchase from Daejung Chemical and Metals Co. Ltd, and nickel nitrate as a dopant, and. Graphene oxide (GO) was bought from Beijing Boyu-Gaoke New Material Technology Co. GO converted into RGO by the annealing process at 500 ºC.TiO_2 paste and ruthenium 535-bis-TBA (N719) were purchase from Solaronix. FTO glass with a sheet resistance of 8X/square and a thickness of 2.2 mm, supplied by Nippon Sheet Glass, was used for both electrodes .The electrolyte produced by a solution of 0.05 M I2, 0.1 M LiI (Adamas-beta), 0.6 M 1-methyl-3-butylimidazolium iodide (TCl), 0.1 m guanidinium thio- cyanate (TCl), and 0.5 M 4-tert-butylpyridine (TCl) mixed in 3-methoxypropionitrile solution (Alfa Aesar). Millipore water (18.25 MΩ cm) was used in the whole process.

1. Photoanode preparation

The Photo electrode (PE) was coated on Fluorine doped tin oxide conducting glass substrate. Firstly the glass was cut with area 2 cm width x 3 cm length and 2.2 mm thickness and cleaned with a number of stages where it is washed with normally water and detergent powder to get rid of the traditional dirt and then placed in distilled water in ultrasonic for 15 min, finally rinsed with ethanol (C_2H_5OH) to remove any traces of greasy stuck and dried.

A thermal blaster has been placed in the edge of the substrate glass covering about 5mm of glass to refine the film on the active area. The TiO_2 paste was fabricated according to (please see ref.[21]).The TiO_2/NiO-RGO nanocomposite was prepared as follows. By the sol-gel process, Nickel nitrate Ni $(NO_3)_2$ was mixed with titanium isopropoxide (TIP) solution during of TiO_2 nanoparticles. The first step, titanium isopropoxide was hydrolyzed with the help of glacial acetic acid (1-2) at 30 º C with addition of 80 mL of ethanol, and the mixture was stirred for 20 min to achieve complete homogeneity. The Ni $(NO_3)_2$ (0.1wt %) was ultrasonically dispersed in 80 mL of deionized water. Then, Ni $(NO_3)_2$ solution was added and stirred for another 10 min to form the suspension solution of TiO_2 nanoparticles. In order to deposit nickel oxide

(NiO) (0.1wt %) onto the surface of the TiO_2 nanoparticles was used as follows: (2 mL of 0.5M) of Sodium borohydride ($NaBH_4$) solution was added to the suspension solution of TiO_2 nanoparticles with stirring at 30°C. The TiO_2/NiO was completed with continuously stirring at 50 ° C for 10 h. While, the second step, graphene oxide (GO) suspension (40 mg) and cetyl trimethylammonium bromide (CTAB, 1g) was stirred in 60 mL of ethanol for 30 min, placed in a 250 mL beaker was added drop wise into the above TiO_2/NiO solution. The gel-containing mixture was formed after complete hydrolysis. The product was dried in a vacuum oven at 80°C overnight. To obtain mixed oxide nanocomposite, the gel material was then calcined in air for 5 min at 500°C.

TiO_2/RGO nanocomposites were synthesized by the same method as described above, except that there was no NiO involved. The paste then deposited in the middle of conducting glass by using doctor-blade method. The paste was propagating using glass rod and repeat this step to obtain a homogenous layer with slightly thicker. The film dried in air for 15 min and then heated in furnace for 30 min at a temperature of 400◦C to obtain a homogeneous crystalline shape. The prepared film is immersed in the dye solution (0.5 mW ruthenium complex dyes prepared by (Di-tetrabutylammonium cis-bis (isothiocyanato) bis (2, 2'-bipyridyl-4, 4'-dicarboxylato) ruthenium (II)) dye sensitizers. (TBA=tetra-butylammonium) in a mixture of acetonitrile-butanol for 24 h at 25 ◦C)[22] then removed,

2. DSSC devices fabrication

To prepare counter electrode ,we used platinum prepared according to (please see ref.[22]) .After preparation the photoanode and counter electrode we combine the two electrodes together in a sandwich manner as show in figure(4).The iodide/tri-iodide electrolyte consists of a solution of (0.05 ml) I_2, (0.1 ml) LiI, (0.6 ml) 1-methyl-3-butylimidazolium iodide (TCl), (0.1 ml) guanidinium thiocyanate (TCl), and (0.5 ml0 4-tert-butylpyridine (TCl) mixed in 3-methoxypropionitrile solution[22] was injected between them.

Finally the current-voltage (I-V) characteristic of complete solar cell was measured by using keithley 2400 digital source meter (keithley –USA).

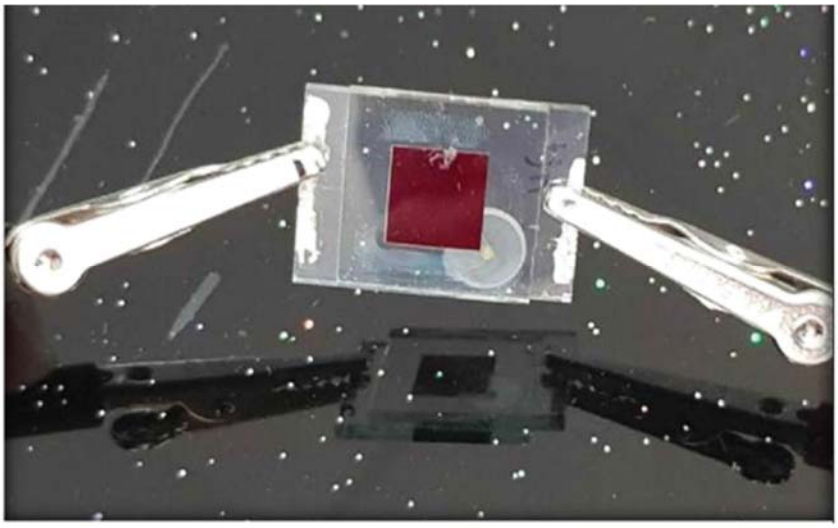

Figure (4): the DSSC device which designed in this work

3. Results and discussion.

The XRD pattern of the TiO_2, NiO, GO and TiO_2/NiO-RGO nanocomposites shows in Figure (5). Major XRD peaks of TiO_2 were observed at 2θ of 36.7°, 38.7 ° and 53.8 °, representing the rutile phase, while the peaks at the 2θ values of 25.5 °, 37.9 °, 48.0 °, 55.1 ° and 62.7 ° indicate the anatase phase of TiO_2 nanoparticles [10], [23] .However, the formation of crystalline NiO on to TiO_2/NiO-RGO nanocomposite was revealed by the diffraction peaks at 2θ values of 37.2 °, 62.7 ° and 75.3 °, indicating that the NiO structure was maintained through the sol-gel process and calcination heat treatment. In the XRD analysis of TiO_2/NiO, the rutile and anatase peaks were observed to be less intense than those for TiO_2. This is due to their large valence difference between Ni^{+2} and Ti^{+4}. In addition , this is can be related to the ionic radius of Ti^{+4} which is very close to that of Ni^{+2}, resulting in more crystal lattice distortion in TiO_2/NiO than in pure TiO_2[24] .In the XRD patterns of the TiO_2/NiO-RGO nanocomposite, no peaks were detected from the RGO surface, indicating that carbonaceous surface was well-exfoliated and covered by TiO_2/NiO metal oxide. The diffraction peaks obtained for TiO_2/NiO-RGO were sharper, reflecting better crystallinity.

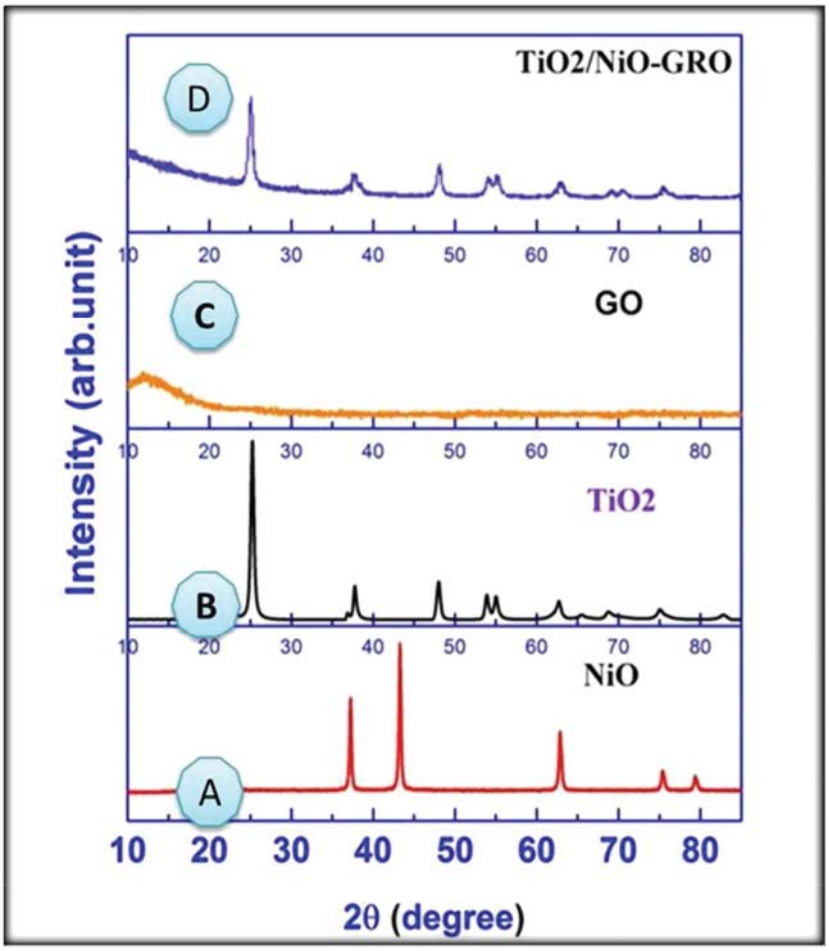

Figure (5): XRD patterns of (A): NiO (B):TiO_2, (C): GO, and (D): TiO_2/NiO-RGO-PE

SEM and EDX analysis of the NiO/RGO and TiO_2/NiO-RGO nanocomposites were shown in figure(6), The SEM graph of TiO_2 is shown in figure (7) which Shows the TiO_2 NPs that has a crisscross-like overlapped pore interceded texture, which is favorable for the absorption and scattering of light [9] TiO_2/NiO

nanoparticles were dispersed and randomly distributed on the surface of the RGO figure 7 (a, b, c). It is suggested that the oxygen-holding functional groups of GO interacted with the OH groups on the surface of the TiO_2/NiO nanoparticles (figure 7d) (before the annealing process) forming the chemically bonded species. The EDX spectra in (figure 7e) show all materials elemental peaks of Ti, O, and Ni were attributed to the TiO_2 and doping of NiO. In addition, the carbon presents for RGO indicates incorporation of Ti and Ni deposited onto the RGO surface

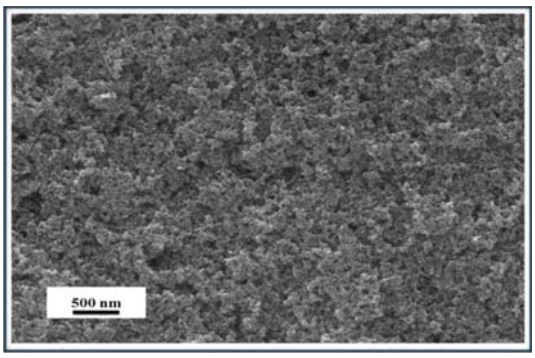

Figure (6): SEM images of synthesized TiO_2 nanoparticles

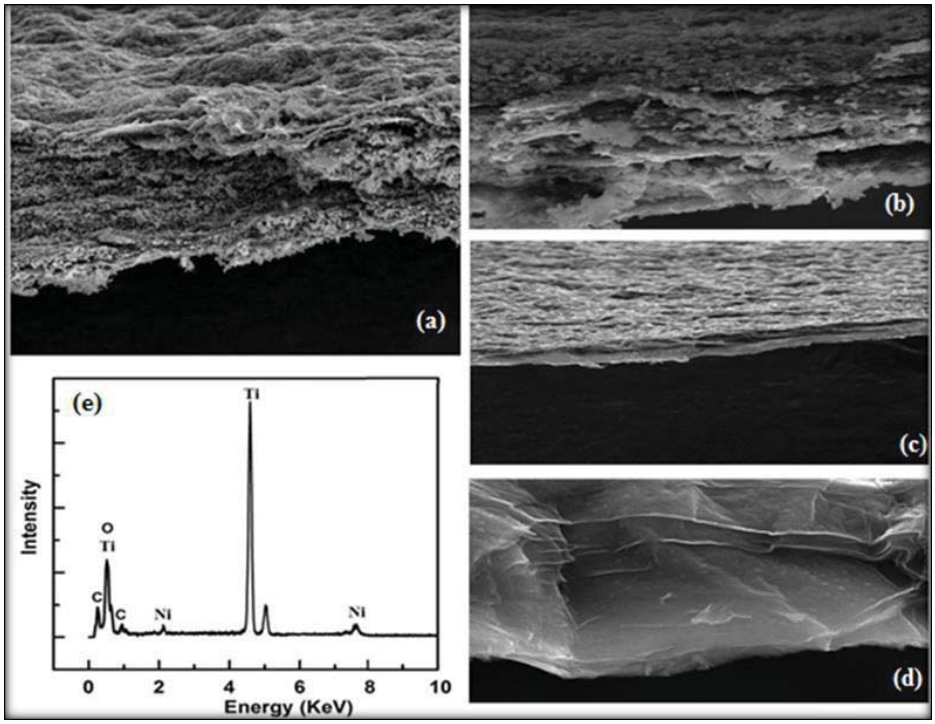

Figure 6: SEM and EDX analysis of TiO_2/NiO-RGO nanocomposite

EIS studies were carried out under illumination of AM 1.5 G (100 mW/cm^2) and using a frequency response analyzer to understand the effect of the electro catalytic activities of CE on the I_3^- reduction. We focus on the semicircle in the highest frequency region describing the electron transport at the CE/electrolyte

interface [4] (Figure8). It's clear in Table (2) that Pt CE has a moderate R_{ct} (1.7Ω), which cause improved electro-catalytic activity for redox electrolyte and high electron-transfer kinetics

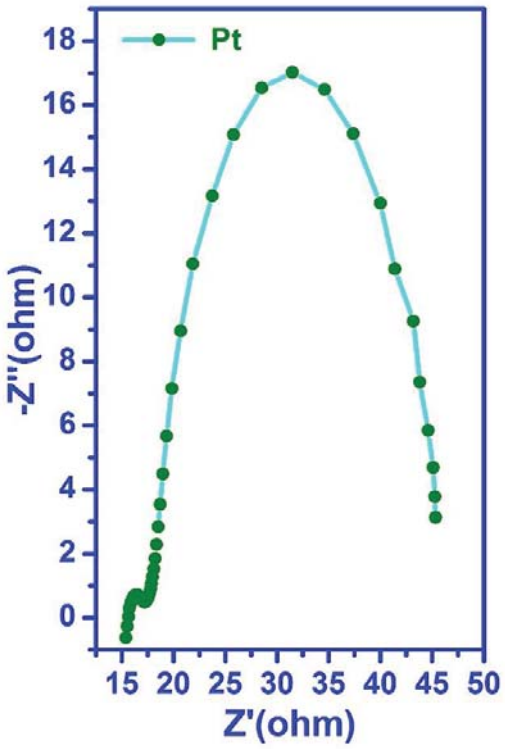

Figure (8): EIS spectra for Pt electrode (a potential amplitude of 10 mV with frequencies from 10 mHz to 100 kHz). The impedance is described either by the real (Z") and imaginary (Z') or by its modulus |Z| and the phase shift ϕ.

Table (1): Epp, Ipa and Ipc of Pt electrodes.

CE	Epp	I_{pa} (mA/cm^2)	I_{pc} (mA/cm^2)
Pt	0.23	0.0023	0.0032

Where Epp is peak to peak separation, Ipa is an anodic peak current density, Ipc is peak-current density. For more understanding of the further the improved DSSC devices with pt-CE we measured CV curves of the I^-/I_3^- redox couple on pt- CE. As shown in figure (9), the oxidation of I^- ions (an anodic peak current density) and the reduction of I_3^- (a cathodic peak current density). As well as, the CE in the DSSC is responsible for catalyzing the regeneration of I^- from I_3^- ($I_3^- + 2e^- \rightarrow 3I^-$)[9]. In addition, it displays a higher peak current density of Pt CE and has a good electro catalytic activity for I^-/I_3^- system

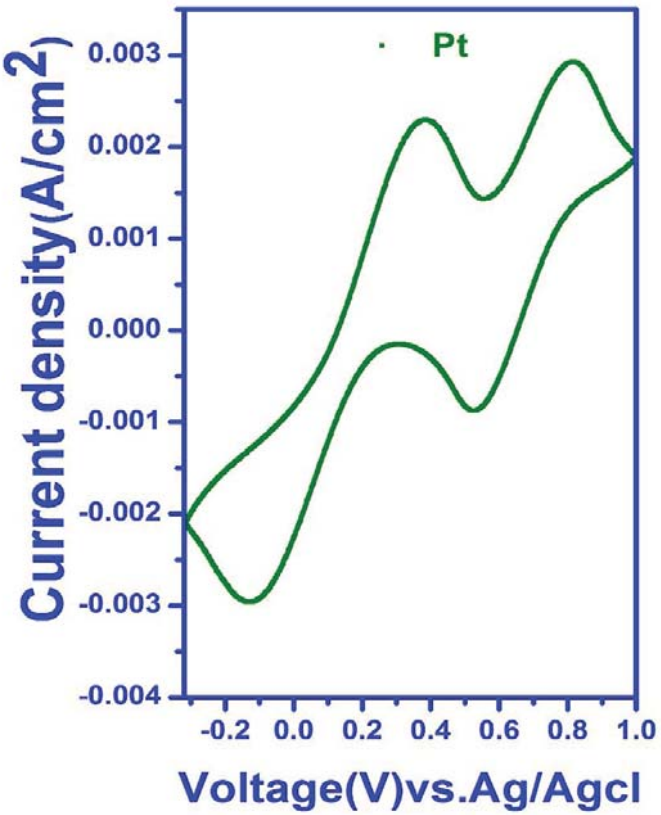

Figure(9): CV for Pt electrode, the electrolyte was acetonitrile solution containing 10 mM LiI, 5 mM I2, and 0.1 M LiClO4. Pt electrode is used as auxiliary electrode and Ag/AgCl works as reference electrode, the scan rate is 50 mV s^{-1}.

Figures 10 and 11, Tables 2 and 3 show I-V curves of the devices based on TiO_2, TiO_2/RGO and TiO_2/NiO-RGO photo electrodes under illumination of AM 1.5 G (100 mW/cm^2) respectively. . The H1 device using pure TiO_2 shows short circuit current density (J_{SC}) of (16.47) mA cm^{-2}, open circuit voltage (V_{OC}) of (0.646) V, fill factor (FF) of (0.632) and power conversion efficiency (η) of (6.69) respectively, which are lower than that of other devices with RGO or NiO/RGO-PEs (Table 2) but H2 and H3 devices performance parameters including Jsc, Voc, FF, and η are summarized in Table 2. The η and FF were calculated according to the eqs:

$$FF = \frac{J_{max} V_{max}}{J_{sc} V_{oc}} \quad (1)$$

$$\eta = \frac{J_{sc} V_{oc} FF}{P_{in}} \times 100 \quad (2) \quad [25]$$

Where J_{max}: is the maximum power current density. V_{max}: maximum power point voltage. J_{sc}: short circuit current density, Voc: open circuit voltage, η: power conversion efficiency, P_{in}: input power. When the H2 and H3 devices have been based on TiO_2/RGO and TiO_2/NiO-RGO photo electrodes,(Table3) the performance has improved remarkably, showing J_{SC} of 16.58 and 17.09 mA cm^{-2}, open circuit voltage V_{OC} of 0.67 and 0.69 V, fill factor FF of 0.66 and 0.6 , conversion efficiency 7.33% and 7.9 respectively. The η significantly enhanced from 6.69 % for H1 device to 7.9 % for H3 device. The H3 devices (figure 10) reach the highest power conversion efficiency due to the charge recombination between photoanode and electrolyte leading to the decreasing performance of devices to a large extent.

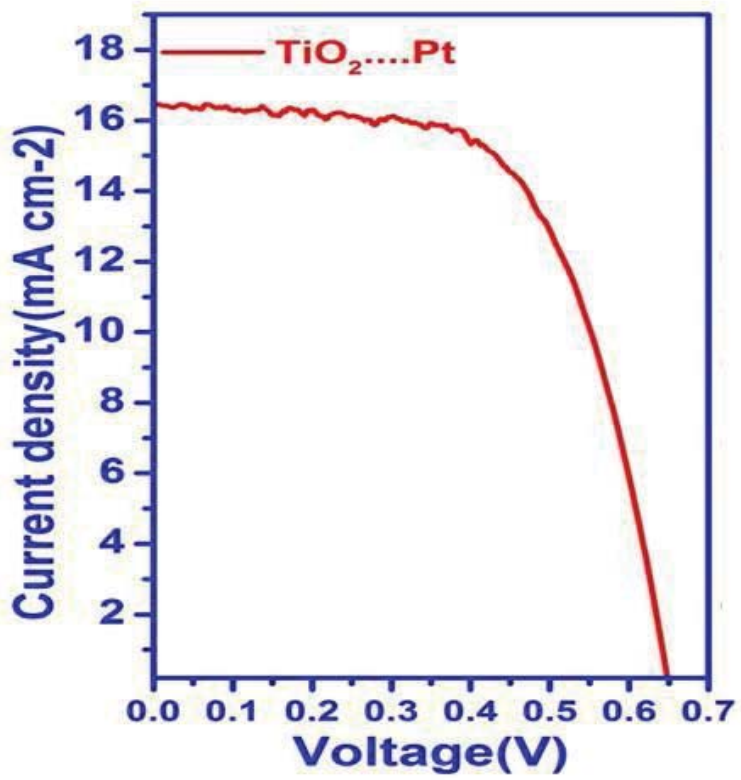

Figure (10): Photocurrent density voltage characteristics of the Pt and NiO-NF/MWCNT.

Table (2): Photovoltaic performance of H1 device.

device	PE	Jsc(mA/cm^2)	V_{oc}(V)	FF	η)%(	R_s(Ω)	R_{ct}(Ω)
H1	TiO_2	16.47	0.646	0.632	6.69	15.6	1.7

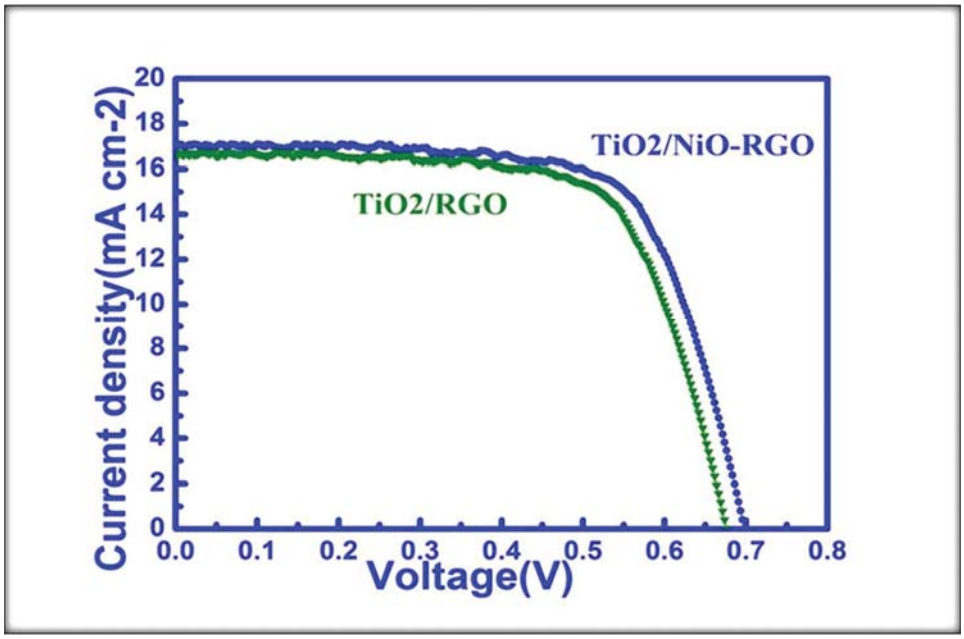

Figure (11): Photocurrent density voltage characteristics of H2and H3

Table3: Photovoltaic performance of H3 and H5 devices.

device	PE	Jsc (mA/cm^2)	V_{oc}(V)	FF	η (%)
H2	TiO_2/RGO	16.58	0.67	0.66	7.33
H3	TiO_2/NiO-RGO	17.09	0.69	0.67	7.9

3.Conclusion

In this paper, films deposited from TiO_2, TiO_2/RGO and TiO_2/RGO-NiO are a prepared by doctor-blade method as a work electrode. Pt is prepared as CE. The DSSCs based on the TiO_2/RGO-NiO nanocomposite electrodes which showed highest photovoltaic performances 7.9% compared with that of the DSSCs made with PEs using TiO_2/RGO and TiO_2 and increased a full factor of 0.67.

References:

[1] B. O'Regan and M. Gratzel, "A Low-Cost, High-Efficiency Solar-Cell Based on Dye-Sensitized Colloidal TiO_2 Films," *Nature*, vol. 353, no. 6346, pp. 737–740, 1991.

[2] K. Nagaveni, M. S. Hegde, N. Ravishankar, G. N. Subbanna, and G. Madras, "Synthesis and Structure of Nanocrystalline TiO 2 with Lower Band Gap Showing High Photocatalytic Activity," *Langmuir*, vol. 20, no. 7, pp. 2900–2907, 2004.

[3] Z. Yang, W. Ahmad, and L. Chu, "Three-dimensional nanocomposite formed by hydrophobic multiwalled carbon nanotubes threading titanium dioxide as the counter electrode," *R. Soc. Chem.*, vol. 55071, no. May, 2016.

[4] M. Raissan Al-Bahrani *et al.*, "NiO-NF/MWCNT nanocomposite catalyst as a counter electrode for high performance dye-sensitized solar cells," *Appl. Surf. Sci.*, vol. 331, pp. 333–338, 2015.

[5] S. Bhatia, *Natural polymer drug delivery systems: Nanoparticles, plants, and algae*. 2016.

[6] J. C. Chou *et al.*, "Photovoltaic Performance Analysis of Dye-Sensitized Solar Cell with ZnO Compact Layer and TiO2/Graphene Oxide Composite Photoanode," *IEEE J. Electron Devices Soc.*, vol. 4, no. 6, pp. 402–409, 2016.
[7] N. Z. Photoelectrode, "Efficient Dye-Sensitized Solar Cells Based on Nanoflower-like ZnO Photoelectrode," *Molecules*, vol. 22, 1284;, no. August 2017, pp. 1–6, 2017.
[8] C.-Y. Lin *et al.*, "Highly efficient dye-sensitized solar cell with a ZnO nanosheet-based photoanode," *Energy Environ. Sci.*, vol. 4, no. 9, p. 3448, 2011.
[9] J. Zhi, A. Chen, H. Cui, Y. Xie, and F. Huang, "NiO-decorated mesoporous TiO2 flowers for an improved photovoltaic dye sensitized solar cell.," *Phys. Chem. Chem. Phys.*, vol. 17, no. 7, pp. 5103–8, 2015.
[10] A. Sharma and B. K. Lee, "Adsorptive/photo-catalytic process for naphthalene removal from aqueous media using in-situ nickel doped titanium nanocomposite," *J. Environ. Manage.*, vol. 155, pp. 114–122, 2015.
[11] L. Wei, S. Chen, Y. Yang, Y. Dong, W. Song, and R. Fan, "Effect of Graphene / TiO 2 Composite Layer on the Performance of Dye-Sensitized Solar Cells," pp. 976–983, 2018.
[12] A. Eshaghi, "solar cell performance Effect of TiO 2 – graphene nanocomposite photoanode on dye-sensitized solar cell performance," no. September 2015, 2016.
[13] L. Wei *et al.*, "Enhanced performance of the dye-sensitized solar cells by the introduction of graphene oxide into the TiO2photoanode," *Inorg. Chem. Front.*, vol. 5, no. 1, pp. 54–62, 2018.
[14] M. Rokhmat, E. Wibowo, Sutisna, Khairurrijal, and M. Abdullah, "Improvement of TiO2/CuO SoPerformancelar Cell by Growing Copper Particle Using Fix Current Electroplating Method," *Procedia Eng.*, vol. 170, pp. 72–77, 2017.
[15] L. B. Patle and A. L. Chaudhari, "Performance of DSSC with Cu Doped TiO2 Electrode Prepared by Dip Coating Technique," vol. 7, no. 8, pp. 1004–1009, 2016.
[16] X. Yang, M. Yanagida, and L. Han, "Reliable evaluation of dye-sensitized solar cells," *Energy Environ. Sci.*, 2013.
[17] M.-H. Jung, M. G. Kang, and M.-J. Chu, "Iodide-functionalized graphene electrolyte for highly efficient dye-sensitized solar cells," *J. Mater. Chem.*, vol. 22, no. 32, p. 16477, 2012.
[18] C. Lee, C. Li, and K. Ho, "Use of organic materials in dye-sensitized solar cells," *Biochem. Pharmacol.*, vol. 20, no. 5, pp. 267–283, 2017.
[19] A. Prasetio, A. M. Habieb, I. Alkian, Z. Arifin, and H. Widiyandari, "Dye-sensitized solar cell based on TiO 2 /MnO 2 composite film as working electrode," *J. Phys. Conf. Ser.*, vol. 877, no. 1, p. 12005, 2017.
[20] H. Wan and H. Wan, "Dye Sensitized Solar Cells," 2004.
[21] W. Sun *et al.*, "Layer-by-Layer Self-Assembly of TiO 2 Hierarchical Nanosheets with Exposed { 001 } Facets As an E ff ective Bifunctional Layer for Dye- Sensitized Solar Cells," *Am. Chem. Soc.*, vol. 10.1021, p. 6, 2014.
[22] M. R. Al-bahrani, W. Ahmad, H. F. Mehnane, Y. Chen, Z. Cheng, and Y. Gao, "Enhanced Electrocatalytic Activity by RGO/MWCNTs/NiO Counter Electrode for Dye-sensitized Solar Cells," *Nano-Micro Lett.*, vol. 7, no. 3, pp. 298–306, 2015.
[23] T. Nguyen-phan, V. Hung, J. Suk, and M. Chhowalla, "Applied Catalysis A : General Photocatalytic performance of Sn-doped TiO 2 / reduced graphene oxide composite materials," *"Applied Catal. A, Gen.*, vol. 473, pp. 21–30, 2014.

[24] M. Cao, P. Wang, Y. Ao, C. Wang, J. Hou, and J. Qian, "Photocatalytic degradation of tetrabromobisphenol A by a," *Chem. Eng. J.*, 2014.
[25] N. Prabavathy, R. Balasundaraprabhu, D. Velauthapillai, and N. Muthukumarasamy, "Enhancement in the photostability of natural dyes for dye-sensitized solar cell (DSSC) applications : a review," no. January, 2017.

[1] B. O'Regan and M. Gratzel, "A Low-Cost, High-Efficiency Solar-Cell Based on Dye-Sensitized Colloidal TiO_2 Films," *Nature*, vol. 353, no. 6346, pp. 737–740, 1991.
[2] K. Nagaveni, M. S. Hegde, N. Ravishankar, G. N. Subbanna, and G. Madras, "Synthesis and Structure of Nanocrystalline TiO 2 with Lower Band Gap Showing High Photocatalytic Activity," *Langmuir*, vol. 20, no. 7, pp. 2900–2907, 2004.
[3] Z. Yang, W. Ahmad, and L. Chu, "Three-dimensional nanocomposite formed by hydrophobic multiwalled carbon nanotubes threading titanium dioxide as the counter electrode," *R. Soc. Chem.*, vol. 55071, no. May, 2016.
[4] M. Raissan Al-Bahrani *et al.*, "NiO-NF/MWCNT nanocomposite catalyst as a counter electrode for high performance dye-sensitized solar cells," *Appl. Surf. Sci.*, vol. 331, pp. 333–338, 2015.
[5] S. Bhatia, *Natural polymer drug delivery systems: Nanoparticles, plants, and algae*. 2016.
[6] J. C. Chou *et al.*, "Photovoltaic Performance Analysis of Dye-Sensitized Solar Cell with ZnO Compact Layer and TiO2/Graphene Oxide Composite Photoanode," *IEEE J. Electron Devices Soc.*, vol. 4, no. 6, pp. 402–409, 2016.
[7] N. Z. Photoelectrode, "Efficient Dye-Sensitized Solar Cells Based on Nanoflower-like ZnO Photoelectrode," *Molecules*, vol. 22, 1284;, no. August 2017, pp. 1–6, 2017.
[8] C.-Y. Lin *et al.*, "Highly efficient dye-sensitized solar cell with a ZnO nanosheet-based photoanode," *Energy Environ. Sci.*, vol. 4, no. 9, p. 3448, 2011.
[9] J. Zhi, A. Chen, H. Cui, Y. Xie, and F. Huang, "NiO-decorated mesoporous TiO2 flowers for an improved photovoltaic dye sensitized solar cell.," *Phys. Chem. Chem. Phys.*, vol. 17, no. 7, pp. 5103–8, 2015.
[10] A. Sharma and B. K. Lee, "Adsorptive/photo-catalytic process for naphthalene removal from aqueous media using in-situ nickel doped titanium nanocomposite," *J. Environ. Manage.*, vol. 155, pp. 114–122, 2015.
[11] L. Wei, S. Chen, Y. Yang, Y. Dong, W. Song, and R. Fan, "Effect of Graphene / TiO 2 Composite Layer on the Performance of Dye-Sensitized Solar Cells," pp. 976–983, 2018.
[12] A. Eshaghi, "solar cell performance Effect of TiO 2 – graphene nanocomposite photoanode on dye-sensitized solar cell performance," no. September 2015, 2016.
[13] L. Wei *et al.*, "Enhanced performance of the dye-sensitized solar cells by the introduction of graphene oxide into the TiO2photoanode," *Inorg. Chem. Front.*, vol. 5, no. 1, pp. 54–62, 2018.
[14] M. Rokhmat, E. Wibowo, Sutisna, Khairurrijal, and M. Abdullah, "Improvement of TiO2/CuO SoPerformancelar Cell by Growing Copper Particle Using Fix Current Electroplating Method," *Procedia Eng.*, vol. 170, pp. 72–77, 2017.
[15] L. B. Patle and A. L. Chaudhari, "Performance of DSSC with Cu Doped TiO2 Electrode Prepared by Dip Coating Technique," vol. 7, no. 8, pp. 1004–1009, 2016.
[16] X. Yang, M. Yanagida, and L. Han, "Reliable evaluation of dye-sensitized solar cells," *Energy Environ. Sci.*, 2013.

[17] M.-H. Jung, M. G. Kang, and M.-J. Chu, "Iodide-functionalized graphene electrolyte for highly efficient dye-sensitized solar cells," *J. Mater. Chem.*, vol. 22, no. 32, p. 16477, 2012.

[18] C. Lee, C. Li, and K. Ho, "Use of organic materials in dye-sensitized solar cells," *Biochem. Pharmacol.*, vol. 20, no. 5, pp. 267–283, 2017.

[19] A. Prasetio, A. M. Habieb, I. Alkian, Z. Arifin, and H. Widiyandari, "Dye-sensitized solar cell based on TiO 2 /MnO 2 composite film as working electrode," *J. Phys. Conf. Ser.*, vol. 877, no. 1, p. 12005, 2017.

[20] H. Wan and H. Wan, "Dye Sensitized Solar Cells," 2004.

[21] W. Sun *et al.*, "Layer-by-Layer Self-Assembly of TiO 2 Hierarchical Nanosheets with Exposed { 001 } Facets As an E ff ective Bifunctional Layer for Dye- Sensitized Solar Cells," *Am. Chem. Soc.*, vol. 10.1021, p. 6, 2014.

[22] M. R. Al-bahrani, W. Ahmad, H. F. Mehnane, Y. Chen, Z. Cheng, and Y. Gao, "Enhanced Electrocatalytic Activity by RGO/MWCNTs/NiO Counter Electrode for Dye-sensitized Solar Cells," *Nano-Micro Lett.*, vol. 7, no. 3, pp. 298–306, 2015.

[23] T. Nguyen-phan, V. Hung, J. Suk, and M. Chhowalla, "Applied Catalysis A : General Photocatalytic performance of Sn-doped TiO 2 / reduced graphene oxide composite materials," *"Applied Catal. A, Gen.*, vol. 473, pp. 21–30, 2014.

[24] M. Cao, P. Wang, Y. Ao, C. Wang, J. Hou, and J. Qian, "Photocatalytic degradation of tetrabromobisphenol A by a," *Chem. Eng. J.*, 2014.

[25] N. Prabavathy, R. Balasundaraprabhu, D. Velauthapillai, and N. Muthukumarasamy, "Enhancement in the photostability of natural dyes for dye-sensitized solar cell (DSSC) applications : a review," no. January, 2017.